Quantitative Aspects of Single Molecule Microscopy

Raimund J. Ober, *Senior Member, IEEE,* Amir Tahmasbi, *Student Member, IEEE,* Sripad Ram,
Zhiping Lin, *Senior Member, IEEE,* and E. Sally Ward

Abstract—Single molecule microscopy is a relatively new optical microscopy technique that allows the detection of individual molecules such as proteins in a cellular context. This technique has generated significant interest among biologists, biophysicists and biochemists, as it holds the promise to provide novel insights into subcellular processes and structures that otherwise cannot be gained through traditional experimental approaches. Single molecule experiments place stringent demands on experimental and algorithmic tools due to the low signal levels and the presence of significant extraneous noise sources. Consequently, this has necessitated the use of advanced statistical signal and image processing techniques for the design and analysis of single molecule experiments. In this tutorial paper, we provide an overview of single molecule microscopy from early works to current applications and challenges. Specific emphasis will be on the quantitative aspects of this imaging modality, in particular single molecule localization and resolvability, which will be discussed from an information theoretic perspective. We review the stochastic framework for image formation, different types of estimation techniques and expressions for the Fisher information matrix. We also discuss several open problems in the field that demand highly non-trivial signal processing algorithms.

I. INTRODUCTION

OPTICAL microscopy has a long history going back several centuries during which it was a key technique for the discovery of biological processes. The basic optical principles have not changed, but what has changed in the instrumentation in recent decades is the availability of highly sensitive detectors, computer control and powerful laser-based light sources [1], [2]. With these improvements in instrumentation came the possibility to analyze the acquired microscopy data using advanced signal and image processing techniques (see e.g. [3], [4]). Equally important, however, are the major advances in molecular biology and physical chemistry that have drastically improved the available technology for the labeling of cellular specimens [5]–[7].

These technological developments coincided with a time when the revolution in molecular biology has demanded powerful exploratory tools for the investigation of molecular processes in cells [1], [7]. For example, through genomic analyses, biologists have identified a large array of proteins, such as growth factor receptors, that are known to play a role in cancer. Standard techniques in molecular biology and biophysics, e.g. X-ray crystallography, allow the study of these proteins to a very high level of detail. However, to investigate their biological functions, it is important that these proteins are studied in their cellular context.

Fluorescence microscopy is the imaging technique of choice for the study of molecular processes within cells due to its ability to detect specifically labeled proteins, receptors, molecules or structures [2], [7], [8]. There are, however, two aspects of fluorescence microscopy that limit its power. The first aspect is the spatial resolution of optical microscopy, which is a measure of the ability to distinguish two closely spaced point-like objects [9]. While molecular interactions occur on the low nanometer scale, classical resolution criteria predict a resolution limit in the range of several hundred nanometers [9]–[11]. The second aspect is the sensitivity of the technique. A fluorescent molecule emits only a limited number of photons [1], [12]. This fact, together with the limited resolution of an optical microscope, implies that in classical fluorescence microscopy only relatively large accumulations of fluorescent molecules are detected. These detection limitations of classical fluorescence microscopy and in particular their associated averaging effects stand in the way of examining the molecular processes and structures at the level of individual molecules, i.e. precisely at the level that is required to study these phenomena in their full detail.

Single molecule microscopy is a technique that promises to overcome the deficiencies of classical fluorescence microscopy by allowing the detection of individual molecules rather than larger accumulations of molecules [1], [12]. Single molecule microscopy goes back to the work by W. E. Moerner and L. Kador published in 1989 [13], followed by that of M. Orrit and J. Bernard published in 1990 [14]. Amongst the many stages of development, we mention a few. In 1991, the image of a single molecule was recorded for the first time [15]. In 2003, single molecule microscopy played a crucial role in the measurement of the step size that the molecular motor myosin V takes in moving along an actin in an in vitro model [16]. This was based on being able to estimate the location of the myosin V molecule within 1.5 nm [16]. The Green Fluorescent Protein (GFP) brought about a major breakthrough in fluorescent microscopy of proteins in living cells as the protein of interest can be genetically tagged by the GFP gene [5], [6]. The first single molecule experiments in live cells using a GFP tag were reported in [17], [18]. In a series of papers, it was recognized that the classical resolution criteria do not apply and distances well below those criteria can be measured using single molecule microscopy [10], [11], [19]. One of the key observations was that resolution is significantly improved if the molecules to be imaged are not excited at the same time [20]. Various photophysical processes were investigated such as blinking [19], photobleaching [11], and
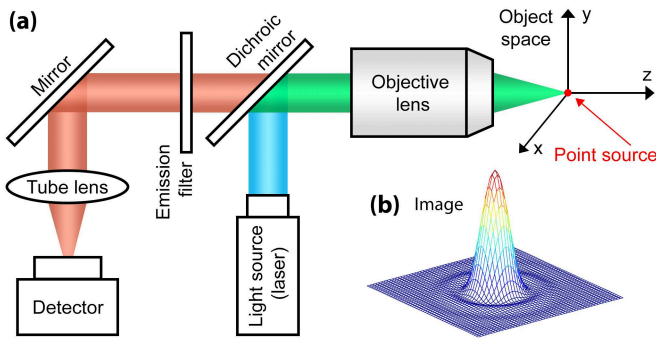
(a)

(b) Image

Fig. 1. The schematic diagram of a basic fluorescence microscopy setup. (a) The excitation light, which is typically generated by a laser, passes through the objective lens to excite the fluorescent molecules in the object space. The fluorescent molecules then emit photons at a specific wavelength that pass through the objective lens, the dichroic mirror and the emission filter, and are then collected by a detector. (b) The mesh plot of the image of an in-focus point source as seen on the detector plane.

photoswitching [21]. This knowledge was exploited in [21]–[23] when it was recognized that various fluorophores can be stochastically excited which allows only a small number of the total fluorophores present in a sample to be imaged at any time point. This led to the development of localization based super-resolution microscopy techniques [21]–[23]. The development of techniques continues at a significant rate with the introduction of new approaches and refinements of existing ones.

This tutorial paper is organized as follows. The next section addresses image formation in a fluorescence microscope as it is relevant for single molecule microscopy. This is followed by a brief explanation of two important types of single molecule experiments, i.e. the tracking experiment and the localization based super-resolution experiment, in Section III. The importance of the location estimation for single molecules will be discussed and appropriate data models will be introduced in Section IV. This will allow us to proceed to address the related parameter estimation problems in Section V. The role the Fisher information matrix and Cramér-Rao lower bound calculations play in the analysis of single molecule experiments will be explored in Section VI, which also contains a discussion of the resolution problem. Extensions to single molecule microscopy in three dimensions and the inherent problems will be the subject of the subsequent section. This is followed by comments on current challenges and concluding remarks.

II. IMAGE FORMATION

Fig. 1(a) shows the schematic of an optical microscope. Excitation light from the light source is reflected off a dichroic mirror and passes through an objective lens to illuminate a fluorescent object (e.g. a point source) that is located in the object space. The fluorescence signal from the object is collected by the same objective lens, then passes through the dichroic mirror and an emission filter, and is then focused on a detector by a tube lens. Image formation in an optical microscope can be described by optical diffraction theory [9]. A fluorophore, i.e. the fluorescent label of a single molecule, is typically modeled as a point source (i.e. a Dirac delta function)

and as such its image is given by the Point Spread Function (PSF), i.e. the impulse response, of the microscope [9]. For an in-focus single molecule, classical diffraction theory predicts that the image can be described by an Airy profile (see Fig. 1(b)) whose analytical expression is given by [9]

$$f(\boldsymbol{r}) = \frac{J_1^2\left(\alpha\left\|\boldsymbol{r}\right\|\right)}{\pi\left\|\boldsymbol{r}\right\|^2}, \qquad \boldsymbol{r} := (x,y) \in \mathbb{R}^2, \qquad (1)$$

where α characterizes the width of the profile, J_1 denotes the first order Bessel function of the first kind, and $\left\|\cdot\right\|$ denotes the Euclidean norm. It is important to note that the Airy profile may not be an accurate model in practice and more advanced PSF models are available (see Section V) [24]–[26]. In addition, as will be discussed in Section VII, the image of an out of focus single molecule depends strongly on the distance from the plane of focus and is distinct from the Airy profile [9], [24]. A fluorescent object can be described as a collection of closely spaced single molecules. As an optical microscope can be modeled as a linear shift-invariant system [9], the image of a fluorescent object is the superposition of the images of point sources at the locations of the single molecules, i.e. the superposition of PSFs, translated according to the locations of the corresponding single molecules.

Most important from our perspective is that the image of a point source is not a point itself but has a non-zero width. Therefore, if there are too many single molecules in close proximity, their images will overlap and the individual single molecules can no longer be differentiated in the image. As a result, in many situations, information about the locations of the single molecules is lost in a fluorescence microscopy image. One of the approaches in single molecule microscopy is therefore to overcome this crowding problem, i.e. to arrange the imaging experiment in such a way that the images of the single molecules are placed sparsely enough so that they can be properly separated. This crowding problem is of course closely related to the notion of resolution that will be the topic of Section VI.

III. LOCALIZATION AND TRACKING EXPERIMENTS

In this section, we discuss the principles behind two of the most important single molecule experiments. The first one, a single molecule tracking experiment, aims at obtaining the trajectories of individual molecules as they move in a cell [3], [4], [27]–[29]. The second one, a localization based super-resolution experiment aims to provide an image with a resolution well beyond what is achievable by classical methods [19], [21]–[23].

A. Tracking single molecules

The movement of molecules such as receptors and proteins in cells is crucial for the functioning of the cells [16], [27]. Despite the importance of these processes much remains unknown. Therefore, tracking experiments, i.e. experiments that record such dynamic behavior over time, are of particular importance [3]. In order to obtain the most detailed analysis, it is essential to carry out these experiments in live cells at the single molecule level (see Fig. 2).
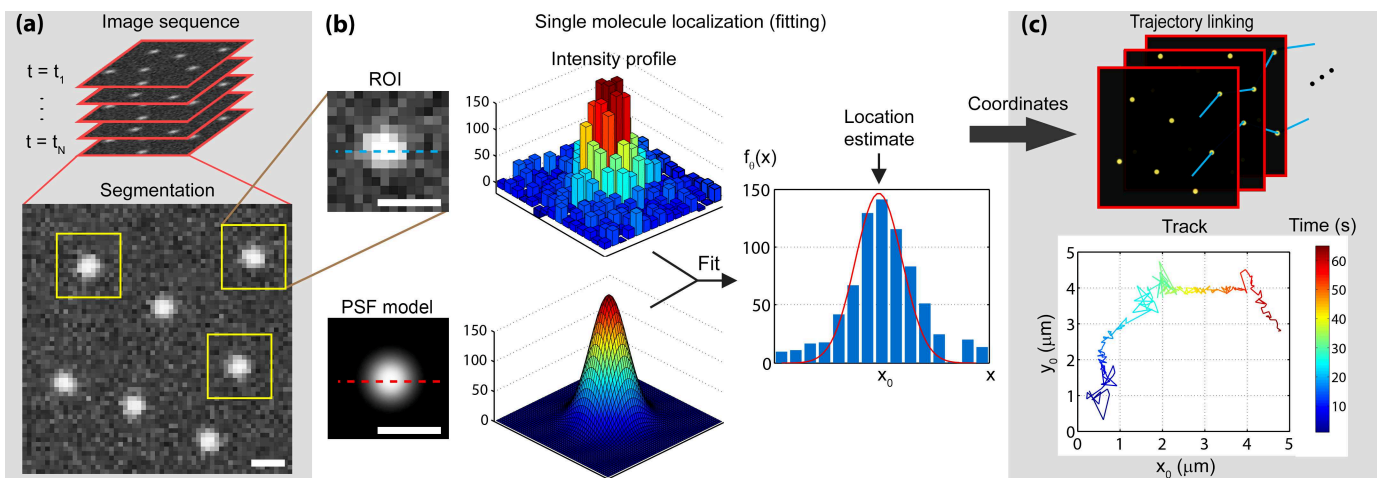
Fig. 2. Single molecule tracking. (a) A sequence of images acquired at different time points are first segmented into multiple Regions of Interest (ROIs) each containing an isolated single molecule. (b) In the single molecule localization step, a PSF model such as the Airy profile or a bivariate Gaussian distribution is fitted to each ROI to estimate the location of the single molecule with sub-pixel precision. This provides a set of coordinates of single molecules. (c) The set of coordinates together with their corresponding time points are then analyzed by a trajectory linking algorithm. In this way, the trajectory of each single molecule can be determined (a sample trajectory is shown). Size bars are 1 μm.

Such single molecule tracking experiments, however, are not without significant challenges. Foremost amongst them is the need to be able to image isolated single molecules [3], [27] (see Fig. 2(a)). This can often be achieved with sparse labeling. Another significant problem is the photobleaching of many of the conventional fluorescent labels, which means that a fluorophore will only emit a certain, typically randomly distributed, number of photons before it ceases to emit photons [5], [6]. The phenomenon in effect limits the length of time for which the track of a single molecule can be followed.

In designing a single molecule tracking experiment a number of important trade-offs need to be made, in particular, regarding the frame rate of the acquisition and the associated exposure time for each of the images. High frame rates and corresponding short exposure times allow for better sampling of the dynamics of the single molecule. Reducing the exposure time, however, decreases the number of photons that are detected during the exposure interval and thereby, as will be shown later, will reduce the accuracy with which the parameters can be estimated that are associated with the trajectory [12], [27], [29]. Increasing the excitation light power could be used to increase the number of emitted photons per exposure. However, this will reduce the lengths of trajectories that can be imaged due to photobleaching. In addition, subjecting a cellular sample to excitation light that is too powerful might damage the living cell that is being imaged.

B. Localization based super-resolution microscopy

The second prototype experiment involves the imaging of fixed, i.e. dead, cells to obtain very high resolution information concerning subcellular structures. In a classical fluorescence microscopy experiment, all fluorophores are simultaneously excited and imaged with one single exposure. As explained earlier, with densely spaced fluorophores, the result is that the individual fluorophores cannot be distinguished in the acquired image (see e.g. Fig. 3(a) and (b)). The idea that underlies localization based super-resolution microscopy is to image the

sample a large number of times, but in each of the images that make up the full acquisition set, only a small and sparse subset of the fluorophores is imaged (see Fig. 3(c)) [21], [22]. Through a particular choice of fluorescent labels, appropriate sample preparation and laser excitation, such sparse, random activation can in fact be achieved. The resulting images each are designed such that the positions of the sparsely located single molecules can be accurately determined. For each of the typically thousands of images, the locations of the single molecules are estimated [22], [23]. The final image is then assembled from the location estimates of the single molecules in each of the images (see Fig. 3(d)).

Different techniques are available to produce these sparse subsets of fluorophores. These are primarily based on the exploitation of new insights into the photophysics of fluorophores [11], [19], [20], whereby powerful excitation light sources can be used to stochastically excite subsets of fluorophores, put them in non-emitting states, or photobleach them. Depending on the specific mechanisms and fluorophores, these techniques are known as Photo-Activated Localization Microscopy (PALM), Stochastic Optical Reconstruction Microscopy (STORM), direct STORM, etc. [21]–[23].

IV. STOCHASTIC DESCRIPTION OF SINGLE MOLECULE DATA

Both the single molecule tracking and the localization based super-resolution experiments depend on the accurate determination of the locations of the imaged single molecules [3], [29], [30]. In order to analyze the algorithmic aspects of the location estimation it is necessary to carefully describe the data generation process that underlies fluorescence microscopy and, in particular, a single molecule experiment. Before introducing a data model for the practical situation in which an image is acquired by a pixelated camera, it is useful to consider an idealized model. In this idealized model, termed the fundamental data model, we assume that the object being imaged emits photons as a Poisson process that are detected
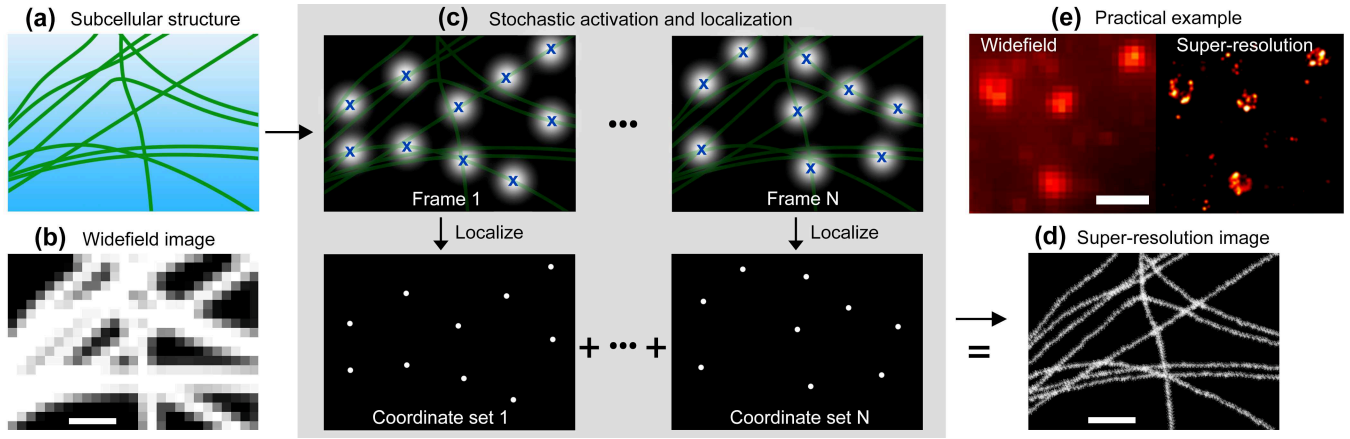
Fig. 3. Localization based super-resolution microscopy. (a) The schematic shows a subcellular structure (a microtubule network) that is uniformly labeled with specific fluorophores. (b) In conventional imaging, all of the fluorophores in the sample are simultaneously excited. Due to the resolution limit of fluorescence microscope, the resulting widefield image is poorly resolved and fails to reveal the underlying structure in the sample. (c) In localization based super-resolution microscopy, the imaging conditions facilitate activation of random subsets of fluorophores that are typically spatially well separated. These fluorophores are then localized with sub-pixel precision and their coordinates are then used to create a super-resolution image of the sample. (d) The resulting super-resolution image provides fine structural information of the sample that is not accessible through a widefield image. (e) Comparison of a practical widefield image and a super-resolution image. In panel (e), the size bar is 2 μm. In all other panels, size bars are 300 nm.

with a rate $\Lambda_\theta(\tau)$, $\tau \geq \tau_0$, on an infinitely large unpixelated detector [12], [31]. In this formulation, $\boldsymbol{\theta} \in \Theta$ denotes the parameter-vector of interest that contains the attributes of the object such as its position, where $\Theta \subseteq \mathbb{R}^n$ is an open parameter space. Making these assumptions allows us to ignore, for the time being, the deteriorating effects due to finite detector size, pixelation and readout noise in the camera [32]. We assume that each photon is detected on the detector at a certain position that is distributed according to a two-dimensional probability distribution $f_{\theta,\tau}(\boldsymbol{r})$, $\boldsymbol{r} = (x,y) \in \mathbb{R}^2$, where $\tau \geq \tau_0$ is the time of detection of the photon [12], [31]. This probability distribution is, in fact, the (continuous) image of the object at the particular time point, normalized such that $\int_{\mathbb{R}^2} f_{\theta,\tau}(\boldsymbol{r})d\boldsymbol{r} = 1$. For instance, this probability distribution can be the Airy profile (see Eq. (1)) or a bivariate Gaussian distribution [9], [12], [31], [33].

As an optical microscope is typically modeled as a linear shift-invariant system [9], the probability distribution function $f_{\theta,\tau}$ can be expressed in terms of an image function q in the following way

$$f_{\theta,\tau}(x,y) = \frac{1}{M^2} q\left(\frac{x}{M} - x_{0,\tau}, \frac{y}{M} - y_{0,\tau}\right), \qquad (2)$$

where $(x,y) \in \mathbb{R}^2$, $M > 0$ denotes the lateral magnification, $(x_{0,\tau}, y_{0,\tau})$ is the position of the object at time $\tau \geq \tau_0$. The image function q describes the image of a stationary object that is located on the optical axis in the object space and is imaged at unit lateral magnification [12], [31]. In the case that the object is a point source, the image function is the same as the PSF of the microscope system.

In practice, the acquired data is corrupted by extraneous noise sources and by the pixelation that is introduced during the capture of the image by an imaging detector. In single molecule experiments, the imaging detector is typically either a Charge Coupled Device (CCD) camera, or Complementary Metal Oxide Semiconductor (CMOS) camera, or an Electron Multiplying CCD (EMCCD) camera [32], [34]. For the time

being, we will concentrate on CCD or CMOS cameras and defer to the end of this section for the discussion regarding EMCCD cameras. We represent a pixelated detector with K_{pix} pixels as $\{C_1, \ldots, C_{K_{pix}}\}$, where $C_k \subseteq \mathbb{R}^2$ denotes the area occupied by the kth pixel of the detector. The acquired data at the kth pixel is given by $\mathcal{I}_{\theta,k} = S_{\theta,k} + B_k + W_k$, $k = 1, \ldots, K_{pix}$.

In the above equation, $S_{\theta,k}$ denotes an independent Poisson random variable with mean $\mu_\theta(k)$ that describes the detected photon count from the object of interest [12], [35], B_k denotes an independent Poisson random variable with mean b_k that describes the photon count due to background and scattering [31], W_k denotes an independent Gaussian random variable with mean η_k and variance σ_k^2 that describes the measurement noise that is introduced during the readout step in the detector [32]. The mean $\mu_\theta(k)$ of the random variable $S_{\theta,k}$ can be expressed in terms of Λ_θ and $f_{\theta,\tau}$, which describe the fundamental data model, and is given by [12], [31]

$$\mu_\theta(k) = \int_{t_1}^{t_2} \int_{C_k} \Lambda_\theta(\tau) f_{\theta,\tau}(\boldsymbol{r}) d\boldsymbol{r} d\tau$$
$$= \frac{1}{M^2} \int_{t_1}^{t_2} \int_{C_k} \Lambda_\theta(\tau) q\left(\frac{x}{M} - x_{0,\tau}, \frac{y}{M} - y_{0,\tau}\right) d\boldsymbol{r} d\tau,$$

for $k = 1, 2, \ldots, K_{pix}$, where $\boldsymbol{r} = (x,y) \in \mathbb{R}^2$, $[t_1, t_2]$ denotes the exposure time interval and we have made use of (2). When the single molecule is stationary, the above equation becomes

$$\mu_\theta(k) = \frac{N}{M^2} \int_{C_k} q\left(\frac{x}{M} - x_0, \frac{y}{M} - y_0\right) d\boldsymbol{r}, \quad k = 1, \ldots, K_{pix},$$

where $N := \int_{t_1}^{t_2} \Lambda_\theta(\tau) d\tau$ denotes the expected number of detected photons on an infinite detector plane [12], [36].

As we will see later, the readout noise in a CCD/CMOS detector can severely impair the quality of the acquired data, especially in the context of low signal levels, i.e. low photon counts. Therefore, over many decades significant efforts have been made to develop image intensifiers that amplify the

signal before the readout process, with the expectation that this will minimize the detrimental effects of the readout noise on the measured signal. This is also the idea behind the EMCCD camera [37] that is widely used in single molecule experiments. The difficulty in analyzing the suitability of this and other amplification based approaches lies in the fact that the amplification process is stochastic, which itself may imply a deterioration of the information content of the signal.

For an EMCCD camera, various probabilistic models have been proposed for the amplification process, which is in fact a branching process [34]. In [37], using a number of approximations, a binomial model was suggested for every stage of the amplification process. For the full process, approximate expressions were also derived for high photon counts in [37]. A comprehensive analysis of the modeling of the EMCCD amplification process was carried out in [34], where several approximate models were also investigated for their accuracy.

V. SINGLE MOLECULE PARAMETER ESTIMATION

The benefits of single molecule microscopy arise from being able to localize single molecules to very high precision [1], [12], [16]. The effective pixel size (i.e. the actual pixel size of the camera chip adjusted for the microscope magnification) in a standard microscope is typically in the range of 65×65 nm^2 to 400×400 nm^2. Localizing a single molecule up to a pixel would not bring any significant advantages, since the localization precision would be of the same order as that of the native resolution of the image [9]–[11], and more importantly biomolecular interactions typically occur at much lower distance scales. Therefore, it is necessary to localize single molecules with sub-pixel precision. This task is far from straightforward due to the often very low signal levels in the presence of significant noise sources, as discussed above [32].

The first attempts were based on elementary approaches such as the center of gravity estimator [28], [38], while current algorithms are primarily based on fitting of a PSF model to the acquired data (see Fig. 2(b)) [28], [33], [36]. The most frequently used fitting criterion is the least-squares criterion [28], although the maximum likelihood estimator is better justified considering the probabilistic model of the acquired data [36]. Specifically, given the measured data $z_1, z_2, \ldots, z_K$ in the pixels that make up the ROI which includes the image of the single molecule, the least squares criterion is given by [28]

$$\hat{\boldsymbol{\theta}} = \operatorname*{argmin}_{\boldsymbol{\theta} \in \Theta} \sum_{k=1}^{K_{pix}} \|z_k - \nu_\theta(k)\|^2,$$

where $\nu_\theta(k) := \mu_\theta(k) + b_k$, and the maximum likelihood criterion is given by [12], [31], [35]

$$\hat{\boldsymbol{\theta}} = \operatorname*{argmax}_{\boldsymbol{\theta} \in \Theta} \ln \, p_{\mathcal{I}_{\theta,1}, \ldots, \mathcal{I}_{\theta,K_{pix}}} \left(z_1, \ldots, z_{K_{pix}} | \boldsymbol{\theta}\right),$$

where $p_{\mathcal{I}_{\theta,1}, \ldots, \mathcal{I}_{\theta,K_{pix}}} \left(z_1, \ldots, z_{K_{pix}} | \boldsymbol{\theta}\right) := \prod_{k=1}^{K_{pix}} p_{\mathcal{I}_{\theta,k}} \left(z_k | \theta\right)$ denotes the joint probability distribution function (pdf) of the observed data. Considering the stochastic framework described in the previous section, for a CCD/CMOS detector, the pdf of the observed data at each pixel, for $k = 1, 2, \ldots, K_{pix}$, is given by [12], [31]

$$p_{\mathcal{I}_{\theta,k}} \left(z_k | \boldsymbol{\theta}\right) = \sum_{j=0}^{\infty} \frac{\nu_\theta(k)^j e^{-\nu_\theta(k)}}{j!} \frac{1}{\sqrt{2\pi}\sigma_k} e^{\frac{-(z_k - j - \eta_k)^2}{2\sigma_k^2}}.$$

The above expression shows that the observed data at each pixel of the detector has a Poisson-Gaussian mixture distribution where, as mentioned earlier, the Poisson and Gaussian parts model the photon detection and readout processes, respectively [31]. See [34] for the pdf for an EMCCD detector.

For the purpose of obtaining a localization based super-resolution image or for the purpose of single molecule tracking, the main information that is necessary from this analysis is the location of the single molecule, i.e. the (x_0, y_0) coordinate. However, often other parameters also need to be estimated to be able to obtain the coordinate estimates. Examples include determining the width parameter of the image profile and the number of detected photons during the acquisition period.

The choice of image profile q in the estimation algorithms raises important questions. As discussed earlier, classical diffraction theory predicts a profile such as the Airy profile. However, very complex PSF models have been advocated to describe optical phenomena such as aberrations [9], [24] and the dipole nature of single molecule [25], [26], [39], or to deal with out of focus situations [9]. On the other hand, it has been argued that in many situations images of single molecules are adequately approximated by 2D Gaussian functions [33], [38], [40] and, therefore, they can be used for estimation purposes. It also needs to be recognized that, especially in the context of biological samples, even if there is a correct model, it is not likely that such a model can be identified with ultimate certainty due to the inherent variability of biological samples. There is also a trade-off between computational complexity and the accuracy of the model of the resulting estimates. For instance, in localization based super-resolution microscopy, typically many tens of thousands of estimates have to be carried out to obtain one image [21], [22] and complex models are typically much more expensive to compute than simpler ones [41].

VI. EVERY PHOTON COUNTS: A FISHER INFORMATION APPROACH TO RESOLUTION AND LOCALIZATION ACCURACY

An important topic in single molecule microscopy has been the question of how well the different single molecule estimation techniques perform in quantitative terms. This is a critical aspect in an experimenter's decision on whether the technique is appropriate for the scientific task, for experiment design and for the evaluation of algorithms. In general terms, there are two aspects that have received significant attention. One is the localization accuracy [12], i.e. the accuracy with which a single molecule can be localized. Second is resolution, loosely speaking the capability of the technique to distinguish different features in the sample [11]. When assessing the performance of a localization algorithm, its mean and standard deviation are most critical. Accuracy of the measurement is paramount even in the context of small data samples. Therefore, ideally unbiased estimators are sought with the lowest

possible standard deviation [35]. While for general estimation problems, it is not always possible to obtain suitable unbiased estimators, many of the estimators that are currently applied in single molecule microscopy, have at least numerically been shown to be unbiased [25], [36]. According to the Cramér-Rao lower bound, the (co)variance (matrix) of any unbiased estimator $\hat{\boldsymbol{\theta}}$ of a parameter (-vector) $\boldsymbol{\theta}$, such as the location parameters, is bounded from below by the inverse of the Fisher information matrix $\boldsymbol{I}(\boldsymbol{\theta})$ [12], [35], i.e.

$$cov(\hat{\boldsymbol{\theta}}) \geq \boldsymbol{I}^{-1}(\boldsymbol{\theta}).$$

The task of assessing the best accuracy with which the various parameters can be estimated therefore reduces to calculating the Fisher information matrix for the specific estimation problem and data model. In [31] a very general expression for the Fisher information matrix was derived for the fundamental data model, i.e. for the ideal case of an infinite detector without pixelation and in the absence of extraneous noise sources. Exploiting the nature of a spatio-temporal marked Poisson process [35], for a general image profile $f_{\theta,\tau}$ and photon detection rate $\Lambda_\theta(\tau)$, $t_1 \leq \tau \leq t_2$, we have [31]

$$\boldsymbol{I}(\boldsymbol{\theta}) = \int_{t_1}^{t_2} \int_{\mathbb{R}^2} \frac{1}{\Lambda_\theta(\tau) f_{\theta,\tau}(\boldsymbol{r})} \left(\frac{\partial \Lambda_\theta(\tau) f_{\theta,\tau}(\boldsymbol{r})}{\partial \boldsymbol{\theta}} \right)^T$$
$$\times \left(\frac{\partial \Lambda_\theta(\tau) f_{\theta,\tau}(\boldsymbol{r})}{\partial \boldsymbol{\theta}} \right) d\boldsymbol{r} d\tau, \qquad \boldsymbol{\theta} \in \Theta.$$

Specializing this expression to the case of a constant photon detection rate, i.e. $\Lambda_\theta(\tau) = \Lambda$, $t_1 \leq \tau \leq t_2$, we immediately obtain that the Fisher information depends linearly on the number of photons detected [12], [31], i.e.

$$\boldsymbol{I}(\boldsymbol{\theta}) = N \int_{\mathbb{R}^2} \frac{1}{f_{\theta,\tau}(\boldsymbol{r})} \left(\frac{\partial f_{\theta,\tau}(\boldsymbol{r})}{\partial \boldsymbol{\theta}} \right)^T \left(\frac{\partial f_{\theta,\tau}(\boldsymbol{r})}{\partial \boldsymbol{\theta}} \right) d\boldsymbol{r}, \, \boldsymbol{\theta} \in \Theta,$$

where $N := (t_2 - t_1)\Lambda$ is the expected number of photons during the exposure interval.

This implies that a lower bound on the standard deviation of the estimate of any parameter (-vector) has the form $\frac{1}{\sqrt{N}}C$, where C is a constant (matrix) related to the specific parameter estimation problem. This is an important aspect of single molecule microscopy. It shows that for algorithms which attain this bound, the accuracy of the parameter estimate depends reciprocally on the square root of the number of collected photons [12], [31].

For the case where the image function is the Airy profile and the single molecule can be assumed to be stationary, it can be shown that this expression implies the following limit on the standard deviation with which the x and y coordinates of the single molecule can be estimated [12]

$$\frac{1}{\sqrt{N}} \frac{\lambda}{2\pi n_a},$$

where λ is the wavelength of the emitted light and n_a is the numerical aperture of the microscope [9]. We refer to this lower bound as the Fundamental Localization Accuracy Measure (FLAM) [36].

The prior expressions are derived assuming the fundamental data model. For the practical data model, where we allow

for a finite pixelated detector, background and readout noise, an expression for the Fisher information matrix can also be derived as follows [34], [36]

$$\boldsymbol{I}(\boldsymbol{\theta}) = \sum_{k=1}^{K_{pix}} \frac{\psi(k)}{\nu_\theta(k)} \left(\frac{\partial \mu_\theta(k)}{\partial \boldsymbol{\theta}} \right)^T \frac{\partial \mu_\theta(k)}{\partial \boldsymbol{\theta}}, \qquad \boldsymbol{\theta} \in \Theta, \quad (3)$$

where $\nu_\theta(k) = \mu_\theta(k) + b_k$ with b_k, $k = 1, \ldots, K_{pix}$, denoting the photon count due to the background noise at pixel C_k. The term $\psi(k)$, $k = 1, \ldots, K_{pix}$, is referred to as the noise coefficient that depends on the type of detector [34]. In the absence of readout noise, $\psi(k) = 1$ for all $k = 1, \ldots, K_{pix}$ [12]. In the presence of readout noise and when using CCD and CMOS detectors, the noise coefficient is given by [31]

$$\psi(k) := \nu_\theta(k)$$
$$\times \left(\frac{e^{-\nu_\theta(k)}}{\sqrt{2\pi}\sigma_k} \int_{\mathbb{R}} \frac{\left(\sum_{l=1}^{\infty} \frac{\nu_\theta^{l-1}(k)}{(l-1)!} e^{\frac{-(z-l-\eta_k)^2}{2\sigma_k^2}} \right)^2}{\sum_{l=0}^{\infty} \frac{\nu_\theta^l(k)}{l!} e^{\frac{-(z-l-\eta_k)^2}{2\sigma_k^2}}} dz - 1 \right),$$

where η_k and σ_k^2 denote the mean and the variance of the readout noise at pixel C_k, $k = 1, 2, \ldots, K_{pix}$, respectively. The expression of the noise coefficient for an EMCCD camera is omitted for brevity but can be found in [34]. Using these expressions, a lower bound can be obtained on the standard deviation with which the x and y coordinates of the single molecule can be estimated in a practical situation. We refer to this lower bound as the Practical Localization Accuracy Measure (PLAM) (see [36]).

These expressions can be used to not only analyze the influence of pixelation, and the various noise sources on the accuracy of the estimates of the location and other parameters. Importantly, these results can also be compared to those based on the fundamental expressions, which give us the theoretically best possible results and thereby let us understand how far a particular experimental configuration is away from the theoretically best possible one. For example, Fig. 4 compares the behavior of the FLAM and PLAM versus the mean photon count and extraneous noise sources for a specific set of imaging conditions.[1] For small photon counts, the PLAM is significantly larger than FLAM implying that pixelation and extraneous noise worsen the localization accuracy whereas for large photon counts the difference is not appreciable (Fig. 4 (a)). In addition, given a certain photon count, increasing the background noise (Fig. 4 (b)) and the readout noise (Fig. 4 (c)) considerably deteriorate the PLAM (when compared with the FLAM).

Another approach to characterize the accuracy with which a single molecule can be localized has been proposed in [38], [42]. Here, using a number of approximations, specific algorithms such as the least squares algorithm have been used, assuming a Gaussian image profile to obtain an expression for the standard deviation of the particular location estimator.

[1]The results can be reproduced using a free software package, the Fand-PLimitTool, available on-line at http://www.wardoberlab.com/software/.

However, great care needs to be taken in the use of these expressions as deviations from the actual performance of the algorithms have been observed when applied to images with Airy profiles [36].

The above analysis, based on the Cramér-Rao lower bound has the advantage that it is independent of any particular estimation algorithm and gives bounds that any unbiased estimator needs to satisfy [31], [35]. From a practical point of view it is, however, important to know how well a particular algorithm performs in comparison to these bounds and whether there is an algorithm that attains the bounds. It is well known that, in general, assessing whether an algorithm attains the Cramér-Rao lower bound or to what extent it differs, is a theoretically difficult question and amenable to a theoretical analysis in only rare cases [35]. For the fundamental data model, in case the image is given by a Gaussian profile, it was shown in [12] that the maximum likelihood estimator reduces to the center of gravity estimator and attains the Cramér-Rao lower bound. For all other cases, no analytical analysis was possible but simulations have shown that the maximum likelihood estimator is consistently close to and in some cases attains the Cramér-Rao lower bound for a wide range of experimental conditions [12], [31], [36].

Classical resolution criteria for microscopy, such as Rayleigh's or Abbé's criterion, are heuristic criteria that were developed at a time when microscope samples were typically investigated by eye, rather than being recorded by a highly sensitive imaging detector [9], [10]. Therefore, the classical notions of resolution did not take into account the added benefits of a detailed analysis of the acquired data by sophisticated image and signal processing algorithms.

Resolution can be defined in a number of ways. One of the most fundamental ones relates to the question of the resolution of two point sources, which is the scenario Rayleigh's classical criterion addresses [9], [11], [43]. It states that two point sources can be resolved if they are separated by a distance of at least $0.61\lambda/n_a$ [9], [10]. Interestingly, this expression does not show any dependence on the amount of data that is acquired. In [11], this two point resolution problem was cast in the above described photon counting framework and the question was changed from "whether or not two points can be resolved" to the question of "how well two points can be resolved". An expression for the limit on the standard deviation with which the distance d between two point sources can be estimated using the fundamental data model was then derived as [11]

$$\sigma_d = \frac{1}{\sqrt{4\pi N \Gamma_0(d)}} \frac{\lambda}{n_a},\qquad(4)$$

where N is the expected photon count on the infinite detector plane per point source and $\Gamma_0(d)$ is a nonlinear function of the distance between point sources (see [11]). Importantly this expression shows that arbitrarily small distances can be resolved, but the smaller the distance, the more photons need to be acquired to obtain the same accuracy. This approach can be generalized to multiple point sources in a relatively straightforward fashion (see e.g. [11], [44]).

The information theoretic resolution measure described above (i.e. (4)) is a powerful tool in determining how well
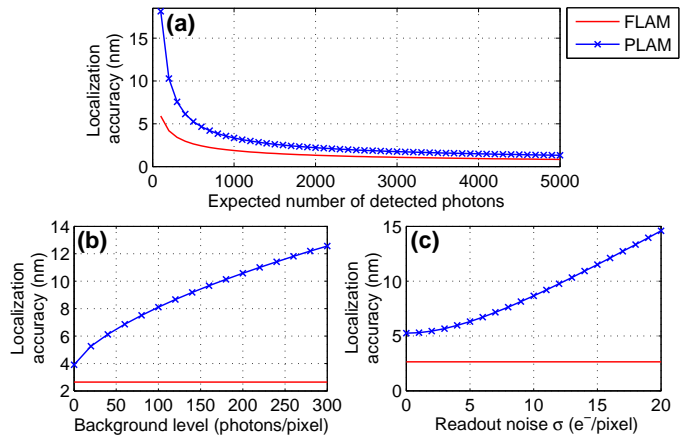

Fig. 4. Single molecule localization measure. Behavior of the localization accuracy using the fundamental data model (i.e. the FLAM) and the practical data model (i.e. the PLAM) for the x-coordinate of the single molecule as a function of (a) the expected number of detected photons N from the single molecule, (b) the background level b_k, and (c) the standard deviation of the readout noise σ_k. For all of the plots, the numerical aperture is set to 1.4, the emission wavelength is set to 520 nm, the lateral magnification is set to 100, the pixel array (ROI) size is set to 25×25 and the pixel dimensions are set to 13×13 μm. In panels (a) and (c), b_k is 20 photons/pixel for all the pixels. In panels (a) and (b), the PLAM is calculated with $\sigma_k = 0$ e$^-$/pixel for all the pixels. In panels (b) and (c), N is set to 500 photons.

two point sources can be resolved, and hence it is suited for applications where the structure of interest can be defined by a limited number of molecules. However, in other applications where continuous structures with a large number of potential labeling sites are imaged, the situation is more complex. One important aspect relates to the labeling density. As shown in [45], with decreasing density of the fluorescent labels, the structure of interest gradually becomes unresolvable in the acquired image, even when the two point resolution measure discussed above is appropriate. A resolution measure based on the Fourier ring correlation was recently published in [46]. This measure can be directly computed from the experimental data and takes into account the localization accuracy, the density of fluorescent labels and the spatial structure of the sample.

VII. Imaging in Three Dimensions

Microscopy is, by its nature, a technique that is most suited to study phenomena that occur in one plane, i.e. the focal plane of the microscope [1], [12]. Cells, however, are three-dimensional (3D) objects, and 3D imaging of cellular processes poses several technical challenges, especially at the single molecule level. In the previous section, we discussed results that showed that the x- and y-coordinates of an in-focus single molecule can be determined with very high accuracy. However, the situation changes dramatically when we are concerned with the estimation of the third spatial coordinate, i.e. the z-position of the single molecule. Considering the standard Born and Wolf 3D PSF model [9], the image function, which now depends on the z_0-position, $z_0 \in \mathbb{R}$, of the single molecule, is given by [27]

$$q_{z_0}(\boldsymbol{r}) = A \left| \int_0^1 J_0\left(\alpha\rho\|\boldsymbol{r}\|\right) e^{j\frac{\pi n_a^2 z_0}{\lambda n_m}\rho^2} \rho \, d\rho \right|^2,\qquad(5)$$
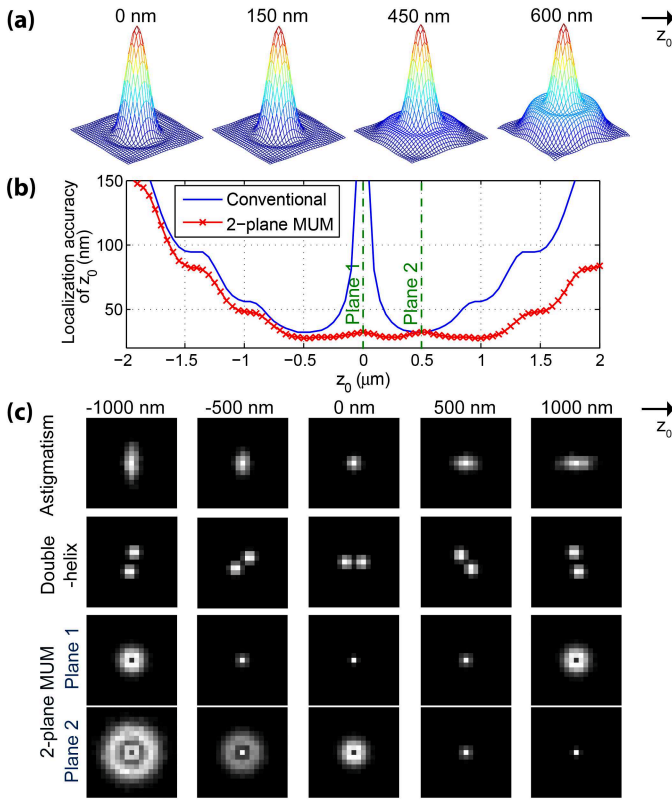
Fig. 5. Single molecule imaging in 3D. (a) Image profile of a point source at different z-positions acquired by a conventional (single plane) microscope. (b) Comparison of the localization accuracy, i.e. the PLAM, for the z-coordinate of the single molecule along the z-axis for a conventional microscope and a 2-plane MUM setup. For a 2-plane MUM setup, the PLAM predicts relatively constant z-localization accuracy for a range of z-positions including at the plane of focus (i.e. $z_0 = 0$). (c) Comparison of 3D single molecule imaging approaches, which encode/deduce the z-position using different strategies.

where $\boldsymbol{r} = (x, y) \in \mathbb{R}^2$, A is a normalization constant, $\alpha := 2\pi n_a/\lambda$, n_m denotes the refractive index of the immersion medium and J_0 is the zeroth order Bessel function of the first kind [9]. As seen in Fig. 5(a), if the single molecule is in focus, i.e. for $z_0 = 0$, the image of the single molecule is identical to the in-focus image we have seen in Fig. 1(b). However, for out of focus positions, i.e. $z_0 \neq 0$, the image starts to depict out of focus rings with increasing z_0 and in general becomes flatter and more spread out.

Using the approaches based on the Cramér-Rao lower bound introduced in Section VI, we can also compute the accuracy with which the z-position of the single molecule can be determined, i.e. the PLAM, (see Fig. 5(b)). Inspecting this plot, we see that far away from the focal plane, i.e. above 1.5 μm, the localization accuracy of the z-coordinate is very poor. Far from the focus, the spread out images are barely visible above the background [27]. It is therefore not surprising that little information can be obtained from them. This indicates that single molecules cannot be satisfactorily localized outside a certain distance from the focal plane.

What may, however, be surprising at first glance is that the accuracy of estimation for the z-position is also very poor when the single molecule is located close to the focal plane (see Fig. 5(b)). The reason for this phenomenon, which we

refer to as the depth discrimination problem, is that, as can be seen in Fig. 5(a), the images of a point source that is located close to the focal plane are barely distinguishable (compare profiles at $z_0 = 0$ and $z_0 = 150$ nm). Therefore, near the focus there is little information in the images of the single molecules about their precise z-positions. The images only start to show appreciable differences when the single molecule is farther from the focal plane (see Fig. 5(a) $z_0 = 450$ and $z_0 = 600$ nm). Aberrations in the sample can reduce the depth discrimination problem [9], [24], [25], but the overall problem persists.

To address the depth discrimination problem, a number of approaches have been proposed. In [47], an astigmatic lens is used which introduces an elongation in the image of the single molecule when it is out of focus. As can be seen in Fig. 5(c), this elongation occurs along different lateral axes depending upon whether the molecule is above or below the plane of focus. By determining the extent of elongation of the image profile, the z-location of the single molecule can be estimated. Approximate analytical expressions are proposed for the PSF of an astigmatic microscope, such as those based on 2D elliptical Gaussian profiles [47].

In another approach [48], sophisticated optical designs have been employed to change the image of a single molecule. The result, shown in Fig. 5(c), is a bimodal image profile, that resembles a double helix and encodes the z-position as a rotation of the profile. The z-location of the single molecule is deduced by determining the change in the relative orientation of the bimodal peaks with respect to the in-focus image. A precise analytical expression is not available for the double helix PSF. Nevertheless, using approximate expressions, the double helix PSF has been shown to provide a relatively uniform z-localization accuracy along the z-axis [48].

A further approach, MUltifocal plane Microscopy (MUM), relies on the simultaneous imaging of several distinct focal planes within the sample (see Fig. 5(c)) [27], [49]. This general approach which is also known by slightly different terminology (e.g. [50], [51]), produces multiple images of a single molecule that are acquired from different depths. The z-location of the single molecule is deduced by simultaneously fitting these images with appropriate 3D PSF models (e.g. (5)). Simultaneous imaging of different focal planes provides consistently more information about the z-position of the single molecule than a conventional microscopy image, even at the plane of focus [27]. This is possible since the Fisher information matrix for a MUM setup $\boldsymbol{I}_{MUM}(\boldsymbol{\theta})$ is the sum of the Fisher information matrices of the individual focal planes $\boldsymbol{I}_k(\boldsymbol{\theta})$, $k = 1, \ldots, K_{pln}$, due to the independence of data acquisition at each focal plane, i.e. we have

$$\boldsymbol{I}_{MUM}(\boldsymbol{\theta}) = \boldsymbol{I}_1(\boldsymbol{\theta}) + \boldsymbol{I}_2(\boldsymbol{\theta}) + \cdots + \boldsymbol{I}_{K_{pln}}(\boldsymbol{\theta}), \qquad \boldsymbol{\theta} \in \Theta.$$

Therefore, the PLAM for MUM shows significant improvements in the z-localization accuracy when compared to a conventional microscope, as shown in Fig. 5(b). Other approaches such as the iPALM are also proposed which rely on interferometric optics [52]. All of the above approaches overcome the depth discrimination problem of conventional microscopy. A possibly competing criterion is related to the range of z-positions over which the single molecule can be

localized to an acceptable accuracy. For a comparison of different 3D imaging modalities see e.g. [53].

VIII. Current challenges

Significant challenges remain in the analysis of single molecule data. One of the assumptions that underlies the localization based super-resolution experiments is that during each acquisition only one single molecule is imaged in a region of interest that allows for the localization of the single molecule [21], [22]. However, since in super-resolution experiments the number of excited fluorophores is stochastic, it cannot be guaranteed that all imaged single molecules are isolated. Therefore, multi-emitters might be present. Hence, there is a significant effort underway to find criteria to determine the number of single molecules in a region of interest and to localize the individual single molecules that are present in the multi-emitter region [44], [54]. It should be pointed out that these problems are highly non-trivial and are closely related to the resolution problem [11].

Additional problems arise from tracking experiments. Often it is assumed that the single molecules are stationary during each of the exposures that are taken to capture the single molecule dynamics. While this can well be an appropriate assumption in many cases, in other experimental situations this is problematic [29]. To analyze this problem, the Fisher information matrix has been calculated in [55] for parameter estimation problems involving a deterministic trajectory during the exposure interval. Diffusion of single molecules on the plasma membrane is an important process that can reveal important biological information [27]. Clearly, diffusive behavior of a single molecule during the exposure of an image can have a significant impact on the resulting image. This process has been investigated in an approximate fashion in a series of papers [29], [56] and approaches have been proposed of how to infer the diffusion coefficient from the obtained images.

As discussed earlier, under specific imaging conditions, e.g. immobilized fluorophores, polarized excitation and out of focus imaging, the dipole nature of a single molecule may become evident in the form of asymmetric image profiles [25], [39], [40]. This can be exploited to estimate the dipole orientation of the fluorophore. However, the analysis of such data is particularly challenging. For example, fitting an inappropriate image profile to the acquired data might lead to biased location estimates [26].

Conventional microscopy produces an image of a sample almost instantly so that the microscopist can immediately evaluate the outcome of the imaging experiment. Localization based super-resolution microscopy experiments, in contrast, require a large number of acquisitions and have a very significant computational overhead, as often images of tens of thousands of single molecules need to be analyzed and processed to produce the final reconstructed image [21], [22]. Single molecule localization can be computationally complex and will therefore by necessity require a non-trivial amount of computational time. In order to make the results of the analysis available to the microscopist as fast as possible, considerable efforts are made to speed up the calculations, for example,

by parallelizing the calculations on Graphics Processing Units (GPUs) [30], [44].

IX. Conclusions

We have reviewed a number of key quantitative aspects of single molecule microscopy. Although this is a nascent field, it has created significant interest amongst biologists, biophysicists and chemists who benefit tremendously from an imaging technique that allows molecular processes to be studied at the level of individual molecules. This new microscopy modality inherently relies on image and signal processing methodologies since the central component of the approach is the precise determination of the positions and other parameters of the imaged single molecules. This localization task is not trivial since the acquired image is characterized by a typically very low photon signal in the presence of significant noise sources. Estimation approaches and expressions for the Cramér-Rao lower bound were reviewed. While much progress has been achieved in a relatively short time, significant problems remain that can benefit from advanced signal processing algorithms.

References

[1] W. E. Moerner, "New directions in single-molecule imaging and analysis," *Proc. Natl. Acad. Sci. USA*, vol. 104, no. 31, pp. 12596–12602, 2007.

[2] J. W. Lichtman and J. Conchello, "Fluorescence microscopy," *Nat. Methods*, vol. 2, no. 12, pp. 910–919, 2005.

[3] E. Meijering, I. Smal, and G. Danuser, "Tracking in molecular bioimaging," *IEEE Signal Process. Mag.*, vol. 23, no. 3, pp. 46–53, 2006.

[4] N. Chenouard *et al.*, "Objective comparison of particle tracking methods," *Nat. Methods*, vol. 11, no. 3, pp. 281–289, 2014.

[5] M. Chalfie, Y. Tu, G. Euskirchen, W. W. Ward, and D. C. Prasher, "Green fluorescent protein as a marker for gene expression," *Science*, vol. 263, no. 5148, pp. 802–805, 1994.

[6] N. C. Shaner *et al.*, "Improved monomeric red, orange and yellow fluorescent proteins derived from Discosoma sp. red fluorescent protein," *Nat. Biotechnol.*, vol. 22, no. 12, pp. 1567–1572, 2004.

[7] X. Michalet *et al.*, "Quantum dots for live cells, in vivo imaging, and diagnostics," *Science*, vol. 307, no. 5709, pp. 538–544, 2005.

[8] D. S. Lidke and K. A. Lidke, "Advances in high-resolution imaging – techniques for three-dimensional imaging of cellular structures," *J. Cell Sci.*, vol. 125, no. 11, pp. 2571–2580, 2013.

[9] M. Born and E. Wolf, *Principles of Optics*, Cambridge Univ. Press, Cambridge, U.K., 1999.

[10] X. Qu, D. Wu, L. Mets, and N. F. Scherer, "Nanometer-localized multiple single-molecule fluorescence microscopy," *Proc. Natl. Acad. Sci. USA*, vol. 101, no. 31, pp. 11298–11303, 2004.

[11] S. Ram, E. S. Ward, and R. J. Ober, "Beyond Rayleigh's criterion: a resolution measure with application to single-molecule microscopy," *Proc. Natl. Acad. Sci. USA*, vol. 103, no. 12, pp. 4457–4462, 2006.

[12] R. J. Ober, S. Ram, and E. S. Ward, "Localization accuracy in single-molecule microscopy," *Biophys. J.*, vol. 86, no. 2, pp. 1185–1200, 2004.

[13] W. E. Moerner and L. Kador, "Optical detection and spectroscopy of single molecules in a solid," *Phys. Rev. Lett.*, vol. 62, no. 21, pp. 2535–2538, 1989.

[14] M. Orrit and J. Bernard, "Single pentacene molecules detected by fluorescence excitation in a p-terphenyl crystal," *Phys. Rev. Lett.*, vol. 65, no. 21, pp. 2716–2719, 1990.

[15] W. P. Ambrose and W. E. Moerner, "Fluorescence spectroscopy and spectral diffusion of single impurity molecules in a crystal," *Nature*, vol. 349, no. 6306, pp. 225–227, 1991.

[16] A. Yildiz *et al.*, "Myosin V walks hand-over-hand: Single fluorophore imaging with 1.5-nm localization," *Science*, vol. 300, no. 5628, pp. 2061–2065, 2003.

[17] R. M. Dickson, A. B. Cubitt, R. Y. Tsien, and W. E. Moerner, "On/off blinking and switching behaviour of single molecules of green fluorescent protein," *Nature*, vol. 388, no. 6640, pp. 355–358, 1997.

[18] R. J. Ober *et al.*, "Exocytosis of IgG as mediated by the receptor, FcRn: an analysis at the single-molecule level," *Proc. Natl. Acad. Sci. USA*, vol. 101, no. 30, pp. 11076–11081, 2004.

[19] K. A. Lidke, B. Rieger, T. M. Jovin, and R. Heintzmann, "Superresolution by localization of quantum dots using blinking statistics," *Opt. Express*, vol. 13, no. 18, pp. 7052–7062, 2005.

[20] A. M. van Oijen, J. Köhler, J. Schmidt, M. Müller, and G. J. Brakenhoff, "3-Dimensional super-resolution by spectrally selective imaging," *Chem. Phys. Lett.*, vol. 292, no. 1–2, pp. 183–187, 1998.

[21] E. Betzig *et al.*, "Imaging intracellular fluorescent proteins at nanometer resolution," *Science*, vol. 313, no. 5793, pp. 1642–1645, 2006.

[22] M. J. Rust, M. Bates, and X. Zhuang, "Sub-diffraction-limit imaging by stochastic optical reconstruction microscopy (STORM)," *Nat. Methods*, vol. 3, no. 10, pp. 793–795, 2006.

[23] S. T. Hess, T. P. K. Girirajan, and M. D. Mason, "Ultra-high resolution imaging by fluorescence photoactivation localization microscopy," *Biophys. J.*, vol. 91, no. 11, pp. 4258–4272, 2006.

[24] S. F. Gibson and F. Lanni, "Experimental test of an analytical model of aberration in an oil-immersion objective lens used in three-dimensional light microscopy," *J. Opt. Soc. Am. A*, vol. 9, no. 1, pp. 154–166, 1992.

[25] F. Aguet *et al.*, "Super-resolution orientation estimation and localization of fluorescent dipoles using 3-D steerable filters," *Opt. Express*, vol. 17, no. 8, pp. 6829–6848, 2009.

[26] M. P. Backlund *et al.*, "The role of molecular dipole orientation in single-molecule fluorescence microscopy and implications for super-resolution imaging," *ChemPhysChem*, vol. 15, no. 4, pp. 587–599, 2014.

[27] S. Ram *et al.*, "High accuracy 3D quantum dot tracking with multifocal plane microscopy for the study of fast intracellular dynamics in live cells," *Biophys. J.*, vol. 95, no. 12, pp. 6025–6043, 2008.

[28] M. K. Cheezum, W. F. Walker, and W. H. Guilford, "Quantitative comparison of algorithms for tracking single fluorescent particles," *Biophys. J.*, vol. 81, no. 4, pp. 2378–2388, 2001.

[29] X. Michalet, "Mean square displacement analysis of single-particle trajectories with localization error: Brownian motion in an isotropic medium," *Phys. Rev. E*, vol. 82, no. 4, pp. 041914, 2010.

[30] C. S. Smith, N. Joseph, B. Rieger, and K. A. Lidke, "Fast, single-molecule localization that achieves theoretically minimum uncertainty," *Nat. Methods*, vol. 7, no. 5, pp. 373–375, 2010.

[31] S. Ram, E. S. Ward, and R. J. Ober, "A stochastic analysis of performance limits for optical microscopes," *Multidim. Sys. Sig. Proc.*, vol. 17, no. 1, pp. 27–57, 2006.

[32] D. L. Snyder *et al.*, "Compensation for readout noise in CCD images," *J. Opt. Soc. Am. A*, vol. 12, no. 2, pp. 272–283, 1995.

[33] B. Zhang, J. Zerubia, and J. -C. Olivo-Marin, "Gaussian approximations of fluorescence microscope point-spread function models," *Appl. Opt.*, vol. 46, no. 10, pp. 1819–1829, 2007.

[34] J. Chao, E. S. Ward, and R. J. Ober, "Fisher information matrix for branching processes with application to electron-multiplying charge-coupled devices," *Multidim. Sys. Sig. Proc.*, vol. 23, no. 3, pp. 349–379, 2012.

[35] D. L. Snyder and M. I. Miller, *Random Point Processes in Time and Space*, 2nd ed. Springer-Verlag, New York, NY, 1991.

[36] A. V. Abraham, S. Ram, J. Chao, E. S. Ward, and R. J. Ober, "Quantitative study of single molecule location estimation techniques," *Opt. Express*, vol. 17, no. 26, pp. 23352–23373, 2009.

[37] J. Hynecek and T. Nishiwaki, "Excess noise and other important characteristics of low light level imaging using charge multiplying CCDs," *IEEE Trans. Electron Devices*, vol. 50, no. 1, pp. 239–245, 2003.

[38] R. E. Thompson, D. R. Larson, and W. W. Webb. "Precise nanometer localization analysis for individual fluorescent probes," *Biophys. J.*, vol. 82, no. 5, pp. 2775–2783, 2002.

[39] J. Enderlein, E. Toprak, and P. R. Selvin, "Polarization effect on position accuracy of fluorophore localization," *Opt. Express*, vol. 14, no. 18, pp. 8111–8120, 2006.

[40] S. Stallinga and B. Rieger, "Accuracy of the Gaussian point spread function model in 2D localization microscopy," *Opt. Express*, vol. 18, no. 24, pp. 24461–24476, 2010.

[41] S. B. Andersson, "Localization of a fluorescent source without numerical fitting," *Opt. Express*, vol. 16, no. 23, pp. 18714–18724, 2008.

[42] N. Bobroff, "Position measurement with a resolution and noise limited instrument," *Rev. Sci. Instrum.*, vol. 57, no. 6, pp. 1152–1157, 1986.

[43] M. Shahram and P. Milanfar, "Imaging below the diffraction limit: a statistical analysis," *IEEE Trans. Image Process.*, vol. 13, no. 5, pp. 677–689, 2004.

[44] F. Huang, S. L. Schwartz, J. M. Byars, and K. A. Lidke, "Simultaneous multiple-emitter fitting for single molecule super-resolution imaging," *Biomed. Opt. Express*, vol. 2, no. 5, pp. 1377–1393, 2011.

[45] H. Shroff, C. G. Galbraith, J. A. Galbraith, and E. Betzig, "Live-cell photoactivated localization microscopy of nanoscale adhesion dynamics," *Nat. Methods*, vol. 5, no. 5, pp. 417–423, 2008.

[46] R. P. J. Nieuwenhuizen *et al.*, "Measuring image resolution in optical nanoscopy," *Nat. Methods*, vol. 10, no. 6, pp. 557–562, 2013.

[47] L. Holtzer, T. Meckel, and T. Schmidt, "Nanometric three-dimensional tracking of individual quantum dots in cells," *Appl. Phys. Lett.*, vol. 90, pp. 053902, 2007.

[48] S. R. P. Pavani and R. Piestun, "Three dimensional tracking of fluorescent microparticles using a photon-limited double-helix response system," *Opt. Express*, vol. 16, no. 26, pp. 22048–22057, 2008.

[49] P. Prabhat, S. Ram, E. S. Ward, and R. J. Ober, "Simultaneous imaging of different focal planes in fluorescence microscopy for the study of cellular dynamics in three dimensions," *IEEE Trans. Nanobiosci.*, vol. 3, no. 4, pp. 237–242, 2004.

[50] S. Abrahamsson *et al.*, "Fast multicolor 3D imaging using aberration-corrected multifocus microscopy," *Nat. Methods*, vol. 10, no. 1, pp. 60–63, 2013.

[51] M. F. Juette *et al.*, "Three-dimensional sub-100 nm resolution fluorescence microscopy of thick samples," *Nat. Methods*, vol. 5, no. 6, pp. 527–529, 2008.

[52] G. Shtengel *et al.*, "Interferometric fluorescent super-resolution microscopy resolves 3D cellular ultrastructure," *Proc. Natl. Acad. Sci. USA*, vol. 106, no. 9, pp. 3125–3130, 2009.

[53] M. Badieirostami, M. D. Lew, M. A. Thompson, and W. E. Moerner, "Three-dimensional localization precision of the double-helix point spread function versus astigmatism and biplane," *Appl. Phys. Lett.*, vol. 97, no. 16, 161103, 2010.

[54] L. Zhu, W. Zhang, D. Elnatan, and B. Huang, "Faster STORM using compressed sensing," *Nat. Methods*, vol. 9, no. 7, pp. 721–723, 2012.

[55] Y. Wong, Z. Lin, and R. J. Ober, "Limits of the accuracy of parameter estimation for moving single molecules imaged by fluorescence microscopy," *IEEE Trans. Signal Prosses.*, vol. 59, no. 3, pp. 895–911, 2011.

[56] X. Michalet and A. J. Berglund, "Optimal diffusion coefficient estimation in single-particle tracking," *Phys. Rev. E*, vol. 85, pp. 061916, 2012.

Raimund J. Ober (S'87-M'88-SM'95) received the Ph.D. degree in electrical engineering from Cambridge University, Cambridge, UK, in 1987. In 1990, he joined the University of Texas at Dallas, Richardson, USA, where he is currently a Professor with the Department of Electrical Engineering. He is also an Adjunct Professor with the University of Texas Southwestern Medical Center at Dallas. His research interests include the development of signal and image processing algorithms for biomedical applications, in particular estimation and tracking for single-molecule microscopy data.

Amir Tahmasbi (S'09) received the B.Sc. and M.Sc. degrees (with honors) both in electrical engineering from Shiraz University of Technology, Shiraz, Iran in 2008 and Iran University of Science and Technology, Tehran, Iran in 2010, respectively. He is currently pursuing his Ph.D. degree in electrical engineering at University of Texas at Dallas, Richardson, USA. His research interests lie in the fields of statistical signal and image processing, and estimation theory with applications to single-molecule microscopy.

Sripad Ram received the B.Sc. degree in applied sciences from PSG College of Technology, Coimbatore, India, in 1999, the M.Sc. degree in physics from the Indian Institute of Technology, Chennai, in 2001 and in 2007, the Ph.D. degree in biomedical engineering from the University of Texas at Arlington and the University of Texas Southwestern Medical Center at Dallas. His research interests include statistical image processing of microscopy data and the development of imaging approaches for 3D tracking of single-molecules.

Zhiping Lin (SM'00) received the Ph.D. degree in information engineering from Cambridge University, Cambridge, UK, in 1987. Since 1999, he has been with the School of Electrical and Electronic Engineering, Nanyang Technological University, Singapore. His research interests include multidimensional systems and signal processing, statistical and biomedical signal processing, and machine learning. He is currently the Editor-in-Chief of Multidimensional Systems and Signal Processing.

E. Sally Ward received the Ph.D. degree from the Department of Biochemistry, Cambridge University, Cambridge, UK, in 1985. In 1990, she joined the University of Texas Southwestern Medical Center at Dallas, USA, where she is a Professor in the Department of Immunology, and currently holds the Paul and Betty Meek-FINA Professorship in Molecular Immunology. Her research interests include antibody engineering, molecular mechanisms that lead to autoimmune disease, questions related to the in vivo dynamics of antibodies, and the development of advanced microscopy techniques.